Title

Internal Fragments Enhance Middle-Down Mass Spectrometry Structural Characterization of Monoclonal Antibodies and Antibody-Drug Conjugates.

Journal

Analytical Chemistry, 96(6)

Authors

Wei, Benqian
Lantz, Carter
Ogorzalek Loo, Rachel
et al.

Publication Date

2024-02-13

DOI

10.1021/acs.analchem.3c04526

Peer reviewed

HHS Public Access

Author manuscript

Anal Chem. Author manuscript; available in PMC 2025 February 13.

Published in final edited form as:

Anal Chem. 2024 February 13; 96(6): 2491–2499. doi:10.1021/acs.analchem.3c04526.

Internal Fragments Enhance Middle-down Mass Spectrometry Structural Characterization of Monoclonal Antibodies and Antibody-drug Conjugates

Benqian Wei[1], **Carter Lantz**[1], **Rachel R. Ogorzalek Loo**[1,3,4], **Iain D. G. Campuzano**[5], **Joseph A. Loo**[1,2,3,4,*]

[1]Department of Chemistry and Biochemistry, University of California Los Angeles-Los Angeles, CA, USA

[2]Department of Biological Chemistry, University of California-Los Angeles, Los Angeles, CA, USA

[3]UCLA-DOE Institute, University of California-Los Angeles, Los Angeles, CA, USA

[4]Molecular Biology Institute, University of California-Los Angeles, Los Angeles, CA, USA

[5]Center for Research Acceleration by Digital Innovation, Molecular Analytics, Amgen Research, Thousand Oaks, CA, USA

Abstract

Monoclonal antibodies (mAbs) and antibody-drug conjugates (ADCs) are important biotherapeutics with large size (~150 kDa) and high structural complexity that require extensive sequence and structure characterization. Middle-down mass spectrometry (MD-MS) is an emerging technique that sequences and maps subunits larger than those released by trypsinolysis. It avoids introducing artifactual modifications that may occur in bottom-up MS, while achieving higher sequence coverage compared to top-down MS. However, returning complete sequence information by MD-MS is still challenging. Here, we show that assigning internal fragments in direct infusion MD-MS of a mAb and an ADC substantially improves their structural characterization. For MD-MS of the reduced NIST mAb, including internal fragments recovers nearly 100% of the sequence by accessing the middle sequence region that is inaccessible by terminal fragments. The identification of important glycosylations can also be improved after

[*]**Corresponding Author Joseph A. Loo** – Department of Chemistry and Biochemistry, University of California Los Angeles, Los Angeles, California 90095, United States; JLoo@chem.ucla.edu.

Benqian Wei – Department of Chemistry and Biochemistry, University of California Los Angeles, Los Angeles, California 90095, United States

Carter Lantz – Department of Chemistry and Biochemistry, University of California, Los Angeles, Los Angeles, California 90095, United States

Rachel R. Ogorzalek Loo – Department of Chemistry and Biochemistry, University of California, Los Angeles, Los Angeles, California 90095, United States

Iain D. G. Campuzano – Amgen Research, Center for Research Acceleration and Digital Innovation, Molecular Analytics, Biologics Therapeutic Discovery, Thousand Oaks, California 91320, United States

Supporting Information

The Supporting Information is available free of charge on the ACS Publications website.

Instrument parameters, ECD cell parameters, and data analysis information; middle-down characterization of the NIST mAb and IgG1-DM1 ADC Fd' and Fc/2 subunits; assignment result of an ECD data of NIST mAb LC subunit; measured sequence coverage of subunits.

The authors declare no competing financial interest.

including internal fragments. For the reduced lysine-linked IgG1-DM1 ADC, we show that considering internal fragments increases the DM1 conjugation sites coverage to 80%, comparable to the reported 83% coverage achieved by peptide mapping on the same ADC.[1] This study expands our work on the application of internal fragment assignments in top-down MS of mAbs and ADCs, and can be extended to other heterogeneous therapeutic molecules such as multispecifics and fusion proteins for more widespread applications.

INTRODUCTION

The first monoclonal antibody (mAb) drug was approved in 1986;[2] since then, mAb-based therapeutics have become increasingly important for the treatment of a host of human diseases including cancer, metabolic disorders, and viral infections.[3-6] The success of mAbs stems from their unique pharmacological properties such as target specificity and affinity, long circulating half-life, and extraordinary safety profiles.[7, 8] MAbs possess high molecular complexity due to their large size (~150 kDa), multiple disulfide bonds within and between light and heavy chains, and a series of post-translational modifications (PTMs)[9-11] that could impact their critical quality attributes (CQAs).[12] Therefore, comprehensive sequence and structure characterization of these intricate molecules as a function of manufacturing and accelerated stability[13-15] is imperative for the production of high quality mAb therapeutics.

In recent years, new mAb formats including nanobodies, fusion proteins, multispecific antibodies, and antibody-drug conjugates (ADCs) have been evolving.[16-18] These formats have enabled new immunotherapy approaches through multitargeting and enhanced antitumor efficacy, of which ADCs have emerged as a promising therapeutic drug classes.[19-23] ADCs couple the target specificity of mAbs with the toxicity of small molecule payloads to enable their “magic bullets” feature, which allows them to selectively kill antigen-expressing targets with higher potency than their mAb counterparts.[24, 25] ADCs are even more heterogeneous molecules than mAbs due to the conjugation of payloads at varying sites, depending on the type of the linker that bridges the payload to the antibody.[22, 26] One common linker strategy targets primary amines (lysine side chains or N-termini), which produces highly heterogeneous nonspecific lysine-linked ADCs in which a large array of locations are conjugated with differing number of payloads.[27-29] Drug conjugation sites are one of the most important CQAs of ADCs because they play a significant role in affecting the physical and pharmaceutical properties of ADCs.[30-32] Therefore, they need to be unambiguously determined to avoid the instances that the conjugation occurs in complementarity-determining regions (CDRs), which could impact the target specificity of lysine-linked ADCs.[1, 33, 34] Robust and reliable analytical techniques need to be established to resolve such molecular heterogeneity.

Among various available analytical techniques, liquid chromatography coupled with mass spectrometry (LC-MS) has been the most popular method routinely used for the characterization of mAbs and ADCs.[35-42] In particular, peptide mapping measures trypsin or Lys-C digested peptides of mAbs/ADCs by reversed phase LC-MS (RPLC-MS).[1, 33, 43-46] This well-established bottom-up approach offers high sequence coverage with amino acid resolution, and can detect low levels of PTMs and identify drug conjugation sites

of ADCs.[47, 48] The development of novel digestion methods to automate and reduce sample handling largely decreases the possibility of introducing artifactual modifications.[47, 49-51] On the other hand, top-down MS (TD-MS) measures intact gas-phase mAb/ADC ions, which minimizes sample preparation and preserves endogenous modifications, but suffers from relatively low fragmentation efficiency for proteins of this large size and high complexity.[34, 52-57]

Middle-down MS (MD-MS) is a promising technique for the characterization of mAbs/ADCs that sequences and maps subunits larger than those released by trypsinolysis.[55, 57-64] It bypasses the digestion step required in bottom-up MS, while achieving higher sequence coverage compared to top-down MS; however, obtaining the same level of sequence and drug conjugation information as peptide mapping remains challenging. Various fragmentation methods have been applied to improve the MD-MS fragmentation efficiency of mAbs and ADCs including collision-,[60, 62, 63] electron-,[55, 57-62, 64] and photon-based dissociation,[55, 57, 60, 62, 64] among which electron-based dissociation (ExD) has shown promising results, particularly with the aid of collisional activation.[55, 57, 60, 64] Typically, such MD-MS experiments involve analyzing ~25 kDa subunits produced by FabRICATOR/reduced treated mAbs/ADCs using online denaturing RPLC-MS. However, ExD MD-MS can require meticulous parameter tuning to achieve optimal fragmentation, rendering online RPLC-MS relatively inefficient and time-consuming due to the need to consider RPLC elution time. An alternative approach is direct infusion MD-MS, which offers higher flexibility in adjusting ExD parameters to maximize fragmentation efficiency.

In addition to applying multiple fragmentation methods, incorporating *internal* fragments into the data analysis workflow represents a viable strategy to enhance sequence information. These noncanonical internal fragments, which arise from multiple cleavage events on the protein backbone,[65] have been demonstrated in previous studies to significantly improve the characterization of proteins,[34, 66-72] protein complexes,[73, 74] and even proteome-wide analysis.[75] Specifically, the inclusion of internal fragment assignments has shown to be valuable in the TD-MS analysis of mAbs and ADCs,[34] which motivates us to explore the employment of internal fragments in MD-MS of mAbs and ADCs to obtain more comprehensive characterization results.[76] A recent study applied MD-MS aided with internal fragment analysis using online denaturing LC-MS/MS to characterize a cysteine-linked therapeutic site-specific ADC, achieving sequence coverages ranging from 70% to 90%.[77]

In this study, we show that assigning internal fragments in native direct infusion MD-MS recovers nearly 100% of the mAb sequence and facilitates the elucidation of various types of N-glycosylations. Notably, this represents the highest sequence coverage of mAbs achieved by methods other than peptide mapping reported to date. For a therapeutic IgG1-DM1 lysine-linked ADC, we successfully determined 80% of all putative DM1 conjugation sites, comparable to the reported 83% coverage achieved by bottom-up peptide mapping on the same ADC.[1] These results highlight the added benefits of analyzing internal fragments in MD-MS and establish MD-MS as a valuable complementary technique to the conventional peptide mapping method for characterizing a variety of therapeutic proteins.

EXPERIMENTAL SECTION

Materials and Reagents.

The humanized IgG1k monoclonal antibody reference material 8671 was purchased from the National Institute of Standards and Technology (NIST, Gaithersburg, MD). The therapeutic ADC supplied by Amgen is an IgG1 covalently conjugated with maytansinoid DM1 payloads on native lysine residues. Details on its preparation and production has been described previously.[1] FabRICATOR (IdeS) protease was purchased from Genovis (Lund, Sweden). Tris-HCl buffer solution (pH 7.5) and tris(2-carboxyethyl)phosphine hydrochloride (TCEP) were acquired from Thermo Fisher Scientific (Bremen, Germany). Ammonium acetate solution (7.5 M) was purchased from Sigma-Aldrich (St. Louis, MO, USA) and diluted to 200 mM.

Sample Preparation.

The mAb and ADC stock samples (10 mg/ml) were diluted in 50 mM Tris-HCl buffer, followed by IdeS digestion (1 unit per μg of mAb/ADC) at 37°C for 1 hour. Subsequently, the IdeS-digested mAb and ADC samples were reduced with 25 mM TCEP in 50 mM Tris-HCl buffer at 37°C for 90 minutes. Additionally, ADC samples were prepared with IdeS digestion alone by treating diluted ADC samples with IdeS protease at a ratio of 1 unit per μg of ADC, with incubation at 37°C for 1 hour. All reduced mAb and ADC samples were buffer exchanged into 200 mM ammonium acetate using Amicon ultra centrifugal filters (10k MWCO) and diluted to a final concentration of ~5-20 μM prior to mass spectrometry measurements.

Native Middle-down Mass Spectrometry.

All reduced samples were directly infused into a Thermo Q Exactive Plus UHMR Orbitrap (Thermo Fisher Scientific, Bremen, Germany) modified with an electromagnetostatic ExD cell (e-MSion Inc., Corvallis, OR) by nanoelectrospray ionization (nESI) using Pt-coated, in-house pulled borosilicate capillaries. The capillary voltage on the nESI source was set between 1.1 and 1.7 kV. The source temperature was set at 250 °C, and the S-lens RF level was set at 200. Other crucial instrument parameters corresponding to ion transmission are listed in Table S1. In the case of NIST mAb subunit fragmentation, individual charge states of the LC subunit (ranging from 6+ to 11+), the Fd' subunit (ranging from 5+ to 9+), and the Fc/2 subunit (ranging from 5+ to 10+) were isolated in the quadrupole using a 20 *m/z* isolation window. For ADC subunit fragmentation, individual charge states of the LC-DM1 subunit (ranging from 7+ to 10+), the Fd'-DM1 subunit (ranging from 7+ to 9+), and the Fc/2-DM1 subunit (ranging from 6+ to 9+) were isolated in the quadrupole using a 60 *m/z* isolation window. Only a singular charge state was isolated each time for subsequent ECD fragmentation. Following isolation, the ions were directed from the ExD cell into the HCD cell, where electron capture dissociation (ECD) took place. Optimization of the ExD cell is described in Figure S1.

Post-ECD collisional activation was applied to minimize the impact of electron capture without dissociation (ECnoD)[53] with collision energy values ranging from 70 to 150V, depending on the isolated charge state. All ECD MS/MS spectra were collected with a noise

threshold set at 3, a resolution of 200,000 at *m/z* 400, AGC target of 1e6, and maximum inject time of 200 ms. Each spectrum was averaged over 100 to 200 scans.

Data Analysis.

Peak Assignments.—All raw MS/MS spectra were deconvoluted using Thermo BioPharma Finder 5.0 (Xtract algorithm). Signal-to-noise ratio (S/N) was varied between 5 to 20 to maximize the ratio of the number of matched fragments to the number of deconvoluted peaks. The resulting deconvoluted mass lists were exported as .csv files for terminal and internal fragment assignment in ClipsMS.[68] Overlapping internal fragments resulting from arrangement and/or frameshift ambiguity[69] were eliminated. Theoretical fragment lists were generated by ProteinProspector v6.4.2.[78] The assignments result of an ECD data of NIST mAb LC subunit is shown as an example in Table S2. Additional information is described in the Supporting Information.

Protein Sequence Coverage.—Protein sequence coverage is determined by dividing the number of observed inter-residue cleavage sites by the total number of inter-residue sites on the protein backbone.

RESULTS AND DISCUSSION

A Native Direct Infusion MD-MS Platform for the Characterization of mAbs and ADCs.

We have developed an innovative native direct infusion MD-MS platform that integrates IdeS digestion and TCEP reduction of mAbs and ADCs with nontraditional ExD fragmentation of direct-infused mAb/ADC subunit ions under native condition (Figure S2). The IdeS protease cleaves antibodies below the hinge region followed by disulfide bond reduction to produce approximately 25 kDa subunits (Figure S2A). Traditionally, these subunits are separated by RPLC, and subsequent MS/MS analysis generates sequence-informative fragment ions.[55, 58, 61, 64] This well-established workflow can be operated with high automation, achieving efficient separation of all distinct reduced subunits and their variants of mAbs or ADCs. However, the use of ECD in RPLC-MS/MS can lead to decreased experiment efficiency due to the need to consider the chromatography run time during the delicate ECD parameter tuning step.

As a result, optimizing ECD fragmentation becomes a time-consuming process. Therefore, we took an alternative approach to directly infuse reduced mAb/ADC subunits under native solution conditions (Figure S2B). Contrary to RPLC-MS/MS, a long-lasting nanoelectrospray provides increased flexibility and efficiency in fine-tuning ECD parameters to maximize fragmentation efficiency. The native condition also ensures that fewer charge states were generated for each subunit, enabling their separation in the *m/z* dimension in a single MS spectrum. Finally, by consolidating all validated ECD data from each isolated charge state (Figure S2C), we aim to design a comprehensive and fast workflow to obtain optimized fragmentation results.

Characterization of NIST mAb Subunits.

All three NIST mAb subunits, LC, Fd', and Fc/2, can be effectively separated by native MS in the *m/z* dimension, allowing their subsequent isolation and ECD fragmentation (Figure 1). Importantly, the major glycosylations occurring on the Fc/2 subunit were identified through native MS (Figure 1B). While these measurements offered a bird's-eye view of the attributes of NIST mAb, it is necessary to unambiguously determine the sequence and PTMs of the antibody by MS/MS, in which internal fragment analysis can play a significant role. To maximize sequence information obtained by MD-MS, ECD was applied on the most abundant charge states of all three subunits (Figures 2, S3, S4). Both terminal and internal fragments were generated by ECD on the NIST LC subunit, with numerous previously unassigned signals now assigned as internal fragment ions (Figure 2A). Notably, internal fragments largely complement the sequence information obtained by terminal fragments, covering the interior sequence that is largely inaccessible to terminal fragments (Figures 2B, 2C). Similar results were observed for the Fd' and Fc/2 subunits, in which the incorporation of internal fragments substantially enhanced sequence information obtained for these subunits (Figures S3, S4).

By incorporating internal fragment assignments, we achieved near complete sequence coverage of NIST mAb LC, Fd', and Fc/2 subunits. Through the integration of one optimized ECD data per charge state for each subunit, the sequence coverage increased from 74% to 95% for the LC subunit, 58% to 92% for the Fd' subunit, and 55% to 92% for the Fc/2 subunit after considering internal fragments (Table S3). Unsurprisingly, this significant improvement is largely due to the ability of internal fragments to access the interior protein sequence. The coverage increased from 76% to 100% for the LC subunit middle region (residues 71-142), 37% to 91% for the Fd' subunit middle region (residues 79-158), and 37% to 89% for the Fc/2 subunit middle region (residues 70-140) with the inclusion of internal fragments. Furthermore, internal fragments possess two cleavage sites on the protein backbone, whereas terminal fragments only cleave the protein once. This difference enables internal fragments to inherently carry more sequence information than terminal fragments, contributing to the enhancement in sequence coverage.

The complementarity-determining regions (CDRs) play a vital role in defining the antigen specificity of mAbs; thus unambiguous determination of their sequences is necessary. In addition, the possible presence of problematic chemical liabilities such as deamidation, isomerization, and oxidation within the CDRs highlights the need to thoroughly characterize the CDRs sequences.[80] Overall, the assignment of internal fragments improved sequence coverages of both LC CDRs, increasing from 70% to 100%, and Fd' CDRs, increasing from 89% to 94%. Only two missed cleavages in CDRs, including K66|D67 within CDR2 of the Fd' subunit, and R99|D100 at the beginning of CDR3 of the Fd' subunit, were observed across all CDRs of the NIST mAb after including internal fragments, and both can be accommodated in different ways. The first missed cleavage at K66|D67, is covered by incorporating adjusted ECD data (*vide infra*), while the second missed cleavage at R99|D100 is complemented by the cleavage occurring at the subsequent site at D100|M101. This cleavage captures any potential chemical liability that may occur at residue D100 as R99 is not part of CDR3 of the Fd' subunit. This demonstrates the power of incorporating

internal fragments to comprehensively and unambiguously determine the CDRs sequence. Lastly, although with little automation and relatively low throughput, the high flexibility of our native direct infusion MD-MS platform allowed for the integration of one or two additional adjusted ECD datasets per charge state of each subunit with minimal time loss. This further increased the sequence coverage of all three subunits even closer to 100% (98% for the LC subunit, 97% for the Fd' subunit, and 97% for the Fc/2 subunit), with only one single missed cleavage observed in the CDRs sequence (Table S4).

In addition to enhancing sequence information, the assignment of internal fragments also contributes to identifying various types of prevalent N-glycosylations. By consolidating one ECD data per charge state, MD-MS of the NIST mAb Fc subunit generated a total of 21 terminal fragments containing G0F (11), G1F (4), and G2F (6) N-glycans, while 33 internal fragments were generated containing these three predominant N-glycosylations, with 19 containing G0F, 8 containing G1F, and 6 containing G2F (Figure S5A). This highlights the value of analyzing internal fragments for N-glycosylation identification. The flexibility of tuning ECD parameters within our native direct infusion MD-MS platform further improved the detection of N-glycosylations. By integrating one or two additional adjusted ECD datasets per charge state, we observed an increase of the number of assigned G0F/G1F/G2F-bound terminal and internal fragments to 42 and 50, respectively (Figure S5B). Furthermore, Lippold and coworkers showed that internal fragments generated from denaturing RPLC MD-MS of individual antibody glycoforms using HCD can be used to assess functional relevant deamidation at Asn 325 both qualitatively and quantitatively.[81] This demonstrates that internal fragments can potentially play a bigger role in identifying and quantifying low-level problematic PTMs such as oxidation or deamidation, as these modifications may not be accessible by terminal fragments.

Characterization of IgG1-DM1 ADC Subunits.

The naked antibody of the IgG1-DM1 ADC used in this study contains a total of 90 putative conjugation sites, including 11 from the LC subunit, 16 from the Fd' subunit, and 18 from the Fc/2 subunit. The large number of potential conjugation sites and the inherent random nature of lysine conjugation result in the high heterogeneity of this ADC. To determine the DM1 conjugation sites of the ADC, we took a similar native direct infusion MD-MS approach by applying ECD on isolated DM1-bound subunit ions of the ADC. However, the close mass similarity between the Fd' and Fc/2 subunits of the antibody used in this ADC makes it challenging to isolate each subunit individually within a single spectrum due to potential peak overlaps. Therefore, we performed two reduction experiments, one involving both IdeS digestion and TCEP reduction (Figures 1C, 1D), and the other with IdeS digestion alone (Figures 1E, 1F), to produce Fd' and Fc/2 subunits separately. Native MS of the reduced ADC offers a global overview of the conjugation level and reveals that DM1 is conjugated to all three subunits of the antibody, confirming the high heterogeneity of this ADC (Figures 1D, 1F). Only 1DM1 binding was observed for all three subunits, possibly due to the native condition they were ionized in. It was observed before that DAR values under native condition are measurably lower than under denaturing condition because conjugates with higher DAR values are more hydrophobic, thus ionize more efficiently under denaturing condition.[82] ECD on all three DM1-bound subunits generated

both terminal and internal fragments as well as their DM1-bound forms, providing direct evidence to determine the DM1 conjugation sites (Figures 3A, S6A, S7A).

Similar to our report on ADC characterization using TD-MS,[34] here we define *localizing a conjugation site* as being able to specify the exact lysine residue where the conjugation occurs, while *identifying a conjugation site* refers to confirming the conjugation on several possible lysine residues without pinpointing the exact one. ECD analysis of the LC subunit generated 24 DM1-bound terminal fragments and 43 DM1-bound internal fragments, enabling the localization of 6 conjugation sites and identification of 3 additional conjugation sites (Figure 3B). Assigning DM1-bound terminal fragments could only identify 2 conjugation sites without localizing any (Figure 3B). In contrast, adding DM1-bound internal fragments allowed us to localize 6 conjugation sites (K46, K67, K106, K114, K133, K190) and identify 3 extra conjugation sites (Figure 3B). Specifically, the conjugation site at K46 was localized by 5 DM1-bound internal fragments ($CZ_{20\text{-}51}$, $CZ_{31\text{-}62}$, $CZ_{37\text{-}53}$, $CZ_{42\text{-}57}$, $CZ_{46\text{-}61}$), K67 by DM1-bound $CZ_{59\text{-}80}$, K106 by DM1-bound $CZ_{104\text{-}109}$, K114 by 3 DM1-bound internal fragments ($CZ_{107\text{-}115}$, $CZ_{108\text{-}127}$, $CZ_{110\text{-}129}$), K133 by DM1-bound $CZ_{118\text{-}136}$, and K190 by DM1-bound $CZ_{184\text{-}206}$ (Figure 3B). Similar results were observed for the Fd' and Fc/2 subunits (Figures S6, S7). ECD of the Fd' subunit generated 35 DM1-bound terminal fragments and 30 DM1-bound internal fragments (Figure S6). Only 2 conjugations sites were identified with terminal fragments alone, whereas 4 conjugation sites were localized (K13, K43, K67, K153) and 5 additional conjugation sites were identified with the inclusion of internal fragments (Figure S6). In the case of Fc subunit, 43 DM1-bound terminal fragments and 72 DM1-bound internal fragments were generated by ECD (Figure S7). The assignment of internal fragments localized 5 conjugations sites (K98, K124, K134, K178, K203) and identified 8 other conjugation sites, significantly improved from 2 identified conjugation sites with terminal fragments alone (Figure S7).

The determination status of each potential conjugation site across all three subunits is summarized in Figure 4. The *identified* but not *localized* conjugation sites were shown as blue-colored residues (*determined*) on the lysine site closest to either terminus for illustration purposes. Terminal fragments mainly determined conjugation sites close to the termini while internal fragments largely improved the determination of interior conjugations sites (Figure 4). In total, the incorporation of internal fragments resulted in the determination of 62 conjugation sites (30 *localized*, 32 *identified*), covering 69% of all putative conjugation sites of the antibody (Table S5). Importantly, the flexibility of our native direct infusion MD-MS system shows promising value for characterizing the IgG1-DM1 ADC. By adding one or two ECD datasets per charge state for each subunit, we increased the number of determined conjugation sites from 62 to 72 (44 *localized*, 28 *identified*), resulting in an 80% DM1 conjugation site coverage (Table S6). This result is comparable to the reported 83% coverage obtained from peptide mapping on the same ADC,[1] demonstrating the immense value of analyzing internal fragments for characterizing ADCs by MD-MS, boosting its performance to a level close to that of peptide mapping. Importantly, the conjugation sites determined in our study are largely complementary to those achieved by peptide mapping (Figure 4, middle row vs. bottom row). For example, K106 on the LC subunit, K127 and K153 on the Fd' subunit, and K102, K134, K173 on the Fc/2 subunit were not determined by peptide mapping, whereas they are determined by our MD-MS workflow (Figure 4).

In contrast, the conjugation sites not determined in our study (K170 and K175 on the LC subunit, K54, K139, K211, K219, K220, K224 on the Fd' subunit, and K52, K54, K84, K86 on the Fc/2 subunit) were all determined by the bottom-up peptide mapping method.[1] It has to be noted that the referred peptide mapping study only utilized trypsin for digestion which may have limited the digestion efficiency because the conjugation of DM1 molecules on lysine residues may affect the enzymatic cleavages on these sites. In this case, chymotrypsin might be a more viable option to digest this ADC. Nevertheless, the complementary conjugation information obtained by our MD-MS system demonstrates the benefits of combining multiple characterization workflows.

CONCLUSIONS

Here we report the primary benefits of including internal fragments for the MD-MS characterization of the NIST mAb and a heterogeneous lysine-linked IgG1-DM1 ADC. We developed a native direct infusion MD-MS platform that provides high flexibility to maximize ECD performance with high efficiency, which is difficult to achieve by traditional MD-MS methods using RPLC. The assignment of internal fragments increases the sequence coverage of all three NIST mAb subunits to nearly 100% by accessing the interior protein sequence that is challenging to probe by terminal fragments. Important N-glycosylation information can be elucidated by analyzing internal fragments, which opens the potential of applying internal fragments to identify other low-level PTMs, such as deamidation, oxidation, isomerization, and other unexpected PTMs. In addition, we show that assigning internal fragments significantly improves the determination of drug conjugation sites of a IgG1-DM1 ADC to achieve an 80% drug conjugation site coverage, comparable to the 83% coverage obtained from a previous report using peptide mapping approach.[1] Importantly, with the integration of internal fragments, our MD-MS workflow provides complementary DM1 conjugation information to peptide mapping. However, caveats still exist in the current workflow. The optimization of ECD conditions for every subunit and charge state as well as the manual validation of all assigned internal fragments not only are labor-intensive, but also require experienced operators. The time needed for the entire workflow also largely limits its throughput, preventing this direct infusion MD-MS platform from being applied for routine analysis of mAbs and ADCs.

The results presented here build upon and demonstrate improvements from our previous work on applying internal fragments for native TD-MS characterization of intact mAbs and ADCs.[34] Although TD-MS offers easier sample preparation, it cannot reach the extensiveness of MD-MS characterization in terms of sequence and drug conjugation coverage. Nonetheless, our TD-MS platform possesses a unique advantage in determining intra-chain disulfide connectivity which cannot be achieved by MD-MS.[34] While bottom-up MS remains a well-established approach in the pharmaceutical industry, the MD-MS platform described in this study achieves comparable results and holds great potential if supported by robust automation (e.g., sample processing, nESI) and informatics tools. These findings highlight the potential of MD-MS and internal fragment analysis to enhance the analytical capabilities of MS-based methodologies in characterizing biotherapeutic proteins. It also features the increasing role that native MS could play in therapeutic protein analysis. If ECD tunning can be more efficient within the LC timeframe in the future, online

denaturing MD-MS can be a higher throughput approach. Furthermore, supported by a previous report that showed the extensive presence of internal fragments in bottom-up proteomics,[83] this study suggests that incorporating internal fragments into the bottom-up MS workflow could enable comprehensive characterization of mAbs and ADCs on a routine basis.

Supplementary Material

Refer to Web version on PubMed Central for supplementary material.

ACKNOWLEDGMENT

J.A.L. and R.R.O.L. acknowledge support from the US National Institutes of Health (R35GM145286) and the US Department of Energy (DE-FC02-02ER63421). C.L. acknowledges support from the Ruth L. Kirschstein National Research Service Award program (GM007185).

REFERENCES

1. Luo Q; Chung HH; Borths C; Janson M; Wen J; Joubert MK; Wypych J, Structural Characterization of a Monoclonal Antibody–Maytansinoid Immunoconjugate. Analytical Chemistry 2016, 88 (1), 695–702. [PubMed: 26629796]
2. Goldstein GJS; Tsai HZ; Cosimi BA; Russell PS; Norman D; Barry J; Shield CF; Cho SI; Levey AS; Burdick JF; Williams GM; Stuart FP; Alexander JW; First R; Helderman JH; Wathen RL; Lordon RE; Sampson D; Levin BS, A Randomized Clinical Trial of OKT3 Monoclonal Antibody for Acute Rejection of Cadaveric Renal Transplants. New England Journal of Medicine 1985, 313 (6), 337–342. [PubMed: 2861567]
3. Schrama D; Reisfeld RA; Becker JC, Antibody targeted drugs as cancer therapeutics. Nature Reviews Drug Discovery 2006, 5 (2), 147–159. [PubMed: 16424916]
4. Bebbington C; Yarranton G, Antibodies for the treatment of bacterial infections: current experience and future prospects. Current Opinion in Biotechnology 2008, 19 (6), 613–619. [PubMed: 19000762]
5. Buss NAPS; Henderson SJ; McFarlane M; Shenton JM; de Haan L, Monoclonal antibody therapeutics: history and future. Current Opinion in Pharmacology 2012, 12 (5), 615–622. [PubMed: 22920732]
6. Weiner GJ, Building better monoclonal antibody-based therapeutics. Nature Reviews Cancer 2015, 15 (6), 361–370. [PubMed: 25998715]
7. Kisalu G, N. K; Idris AH; Weidle C; Flores-Garcia Y; Flynn BJ; Sack BK; Murphy S; Schön A; Freire E; Francica JR; Miller AB; Gregory J; March S; Liao H-X; Haynes BF; Wiehe K; Trama AM; Saunders KO; Gladden MA; Monroe A; Bonsignori M; Kanekiyo M; Wheatley AK; McDermott AB; Farney SK; Chuang G-Y; Zhang B; Kc N; Chakravarty S; Kwong PD; Sinnis P; Bhatia SN; Kappe SHI; Sim BKL; Hoffman SL; Zavala F; Pancera M; Seder RA, A human monoclonal antibody prevents malaria infection by targeting a new site of vulnerability on the parasite. Nature Medicine 2018, 24 (4), 408–416.
8. Walsh G; Walsh E, Biopharmaceutical benchmarks 2022. Nature Biotechnology 2022, 40 (12), 1722–1760.
9. Beck A; Wurch T; Bailly C; Corvaia N, Strategies and challenges for the next generation of therapeutic antibodies. Nature Reviews Immunology 2010, 10 (5), 345–352.
10. Liu H; May K, Disulfide bond structures of IgG molecules. mAbs 2012, 4 (1), 17–23. [PubMed: 22327427]
11. Nimmerjahn F; Vidarsson G; Cragg MS, Effect of posttranslational modifications and subclass on IgG activity: from immunity to immunotherapy. Nature Immunology 2023.
12. Rathore AS; Winkle H, Quality by design for biopharmaceuticals. Nature Biotechnology 2009, 27 (1), 26–34.

13. Lowe D; Dudgeon K; Rouet R; Schofield P; Jermutus L; Christ D, Aggregation, stability, and formulation of human antibody therapeutics. In Advances in Protein Chemistry and Structural Biology, Donev R, Ed. Academic Press: 2011; Vol. 84, pp 41–61. [PubMed: 21846562]
14. Kerr RA; Keire DA; Ye H, The impact of standard accelerated stability conditions on antibody higher order structure as assessed by mass spectrometry. mAbs 2019, 11 (5), 930–941. [PubMed: 30913973]
15. Kaur H., Stability testing in monoclonal antibodies. Critical Reviews in Biotechnology 2021, 41 (5), 692–714. [PubMed: 33596751]
16. Husain B; Ellerman D, Expanding the Boundaries of Biotherapeutics with Bispecific Antibodies. BioDrugs 2018, 32 (5), 441–464. [PubMed: 30132211]
17. Grilo AL; Mantalaris A, The Increasingly Human and Profitable Monoclonal Antibody Market. Trends in Biotechnology 2019, 37 (1), 9–16. [PubMed: 29945725]
18. Khongorzul P; Ling CJ; Khan FU; Ihsan AU; Zhang J, Antibody–Drug Conjugates: A Comprehensive Review. Molecular Cancer Research 2020, 18 (1), 3–19. [PubMed: 31659006]
19. Sliwkowski MX; Mellman I, Antibody Therapeutics in Cancer. Science 2013, 341 (6151), 1192–1198. [PubMed: 24031011]
20. Kaplon H; Crescioli S; Chenoweth A; Visweswaraiah J; Reichert JM, Antibodies to watch in 2023. mAbs 2023, 15 (1), 2153410. [PubMed: 36472472]
21. Peters C; Brown S, Antibody–drug conjugates as novel anti-cancer chemotherapeutics. Bioscience Reports 2015, 35 (4), e00225. [PubMed: 26182432]
22. Abdollahpour-Alitappeh M; Lotfinia M; Gharibi T; Mardaneh J; Farhadihosseinabadi B; Larki P; Faghfourian B; Sepehr KS; Abbaszadeh-Goudarzi K; Abbaszadeh-Goudarzi G; Johari B; Zali MR; Bagheri N, Antibody–drug conjugates (ADCs) for cancer therapy: Strategies, challenges, and successes. Journal of Cellular Physiology 2019, 234 (5), 5628–5642. [PubMed: 30478951]
23. Maecker H; Jonnalagadda V; Bhakta S; Jammalamadaka V; Junutula JR, Exploration of the antibody–drug conjugate clinical landscape. mAbs 2023, 15 (1), 2229101. [PubMed: 37639687]
24. Chari RVJ; Miller ML; Widdison WC, Antibody–Drug Conjugates: An Emerging Concept in Cancer Therapy. Angewandte Chemie International Edition 2014, 53 (15), 3796–3827. [PubMed: 24677743]
25. Tsuchikama K; An Z, Antibody-drug conjugates: recent advances in conjugation and linker chemistries. Protein & Cell 2018, 9 (1), 33–46. [PubMed: 27743348]
26. Beck A; Goetsch L; Dumontet C; Corvaïa N, Strategies and challenges for the next generation of antibody–drug conjugates. Nature Reviews Drug Discovery 2017, 16 (5), 315–337. [PubMed: 28303026]
27. Ricart AD, Antibody-Drug Conjugates of Calicheamicin Derivative: Gemtuzumab Ozogamicin and Inotuzumab Ozogamicin. Clinical Cancer Research 2011, 17 (20), 6417–6427. [PubMed: 22003069]
28. Lambert JM; Chari RVJ, Ado-trastuzumab Emtansine (T-DM1): An Antibody–Drug Conjugate (ADC) for HER2-Positive Breast Cancer. Journal of Medicinal Chemistry 2014, 57 (16), 6949–6964. [PubMed: 24967516]
29. Haque M; Forte N; Baker JR, Site-selective lysine conjugation methods and applications towards antibody–drug conjugates. Chemical Communications 2021, 57 (82), 10689–10702. [PubMed: 34570125]
30. Junutula JR; Raab H; Clark S; Bhakta S; Leipold DD; Weir S; Chen Y; Simpson M; Tsai SP; Dennis MS; Lu Y; Meng YG; Ng C; Yang J; Lee CC; Duenas E; Gorrell J; Katta V; Kim A; McDorman K; Flagella K; Venook R; Ross S; Spencer SD; Lee Wong W; Lowman HB; Vandlen R; Sliwkowski MX; Scheller RH; Polakis P; Mallet W, Site-specific conjugation of a cytotoxic drug to an antibody improves the therapeutic index. Nature Biotechnology 2008, 26 (8), 925–932.
31. Shen B-Q; Xu K; Liu L; Raab H; Bhakta S; Kenrick M; Parsons-Reponte KL; Tien J; Yu S-F; Mai E; Li D; Tibbitts J; Baudys J; Saad OM; Scales SJ; McDonald PJ; Hass PE; Eigenbrot C; Nguyen T; Solis WA; Fuji RN; Flagella KM; Patel D; Spencer SD; Khawli LA; Ebens A; Wong WL; Vandlen R; Kaur S; Sliwkowski MX; Scheller RH; Polakis P; Junutula JR, Conjugation site modulates the in vivo stability and therapeutic activity of antibody-drug conjugates. Nature Biotechnology 2012, 30 (2), 184–189.

32. Afar DEH; Bhaskar V; Ibsen E; Breinberg D; Henshall SM; Kench JG; Drobnjak M; Powers R; Wong M; Evangelista F; O'Hara C; Powers D; DuBridge RB; Caras I; Winter R; Anderson T; Solvason N; Stricker PD; Cordon-Cardo C; Scher HI; Grygiel JJ; Sutherland RL; Murray R; Ramakrishnan V; Law DA, Preclinical validation of anti-TMEFF2-auristatin E–conjugated antibodies in the treatment of prostate cancer. Molecular Cancer Therapeutics 2004, 3 (8), 921–932. [PubMed: 15299075]
33. Sang H; Lu G; Liu Y; Hu Q; Xing W; Cui D; Zhou F; Zhang J; Hao H; Wang G; Ye H, Conjugation site analysis of antibody-drug-conjugates (ADCs) by signature ion fingerprinting and normalized area quantitation approach using nano-liquid chromatography coupled to high resolution mass spectrometry. Analytica Chimica Acta 2017, 955, 67–78. [PubMed: 28088282]
34. Wei B; Lantz C; Liu W; Viner R; Ogorzalek Loo RR; Campuzano IDG; Loo JA, Added Value of Internal Fragments for Top-Down Mass Spectrometry of Intact Monoclonal Antibodies and Antibody–Drug Conjugates. Analytical Chemistry 2023, 95 (24), 9347–9356. [PubMed: 37278738]
35. Bobály B; Fleury-Souverain S; Beck A; Veuthey J-L; Guillarme D; Fekete S, Current possibilities of liquid chromatography for the characterization of antibody-drug conjugates. Journal of Pharmaceutical and Biomedical Analysis 2018, 147, 493–505. [PubMed: 28688616]
36. Wakankar A; Chen Y; Gokarn Y; Jacobson FS, Analytical methods for physicochemical characterization of antibody drug conjugates. mAbs 2011, 3 (2), 161–172. [PubMed: 21441786]
37. Zhu X; Huo S; Xue C; An B; Qu J, Current LC-MS-based strategies for characterization and quantification of antibody-drug conjugates. Journal of Pharmaceutical Analysis 2020, 10 (3), 209–220. [PubMed: 32612867]
38. Fekete S; Guillarme D; Sandra P; Sandra K, Chromatographic, Electrophoretic, and Mass Spectrometric Methods for the Analytical Characterization of Protein Biopharmaceuticals. Analytical Chemistry 2016, 88 (1), 480–507. [PubMed: 26629607]
39. Graf T; Heinrich K; Grunert I; Wegele H; Haberger M; Bulau P; Leiss M, Recent advances in LC–MS based characterization of protein-based bio-therapeutics – mastering analytical challenges posed by the increasing format complexity. Journal of Pharmaceutical and Biomedical Analysis 2020, 186, 113251. [PubMed: 32251978]
40. Yang F; Zhang J; Buettner A; Vosika E; Sadek M; Hao Z; Reusch D; Koenig M; Chan W; Bathke A; Pallat H; Lundin V; Kepert JF; Bulau P; Deperalta G; Yu C; Beardsley R; Camilli T; Harris R; Stults J, Mass spectrometry-based multi-attribute method in protein therapeutics product quality monitoring and quality control. mAbs 2023, 15 (1).
41. Dillon TM; Bondarenko PV; Rehder DS; Pipes GD; Kleemann GR; Ricci MS, Optimization of a reversed-phase high-performance liquid chromatography/mass spectrometry method for characterizing recombinant antibody heterogeneity and stability. Journal of Chromatography A 2006, 1120 (1), 112–120. [PubMed: 16448656]
42. Campuzano IDG; Pelegri-O'Day EM; Srinivasan N; Lippens JL; Egea P; Umeda A; Aral J; Zhang T; Laganowsky A; Netirojjanakul C, High-Throughput Mass Spectrometry for Biopharma: A Universal Modality and Target Independent Analytical Method for Accurate Biomolecule Characterization. Journal of the American Society for Mass Spectrometry 2022, 33 (11), 2191–2198. [PubMed: 36206542]
43. Bongers J; Cummings JJ; Ebert MB; Federici MM; Gledhill L; Gulati D; Hilliard GM; Jones BH; Lee KR; Mozdzanowski J; Naimoli M; Burman S, Validation of a peptide mapping method for a therapeutic monoclonal antibody: what could we possibly learn about a method we have run 100 times? Journal of Pharmaceutical and Biomedical Analysis 2000, 21 (6), 1099–1128. [PubMed: 10708395]
44. Song Y; Gao J; Meng Q; Tang F; Wang Y; Zeng Y; Huang W; Shao H; Zhou H, Conjugation site characterization of antibody–drug conjugates using electron-transfer/higher-energy collision dissociation (EThcD). Analytica Chimica Acta 2023, 1251, 340978. [PubMed: 36925279]
45. Ayoub D; Bertaccini D; Diemer H; Wagner-Rousset E; Colas O; Cianférani S; Van Dorsselaer A; Beck A; Schaeffer-Reiss C, Characterization of the N-Terminal Heterogeneities of Monoclonal Antibodies Using In-Gel Charge Derivatization of α-Amines and LC-MS/MS. Analytical Chemistry 2015, 87 (7), 3784–3790. [PubMed: 25769014]

46. Janin-Bussat M-C; Dillenbourg M; Corvaia N; Beck A; Klinguer-Hamour C, Characterization of antibody drug conjugate positional isomers at cysteine residues by peptide mapping LC–MS analysis. Journal of Chromatography B 2015, 981-982, 9–13.
47. Richardson J; Zhang Z, Fully Unattended Online Protein Digestion and LC–MS Peptide Mapping. Analytical Chemistry 2023, 95 (42), 15514–15521. [PubMed: 37816151]
48. Wang Y; Li X; Liu Y-H; Richardson D; Li H; Shameem M; Yang X, Simultaneous monitoring of oxidation, deamidation, isomerization, and glycosylation of monoclonal antibodies by liquid chromatography-mass spectrometry method with ultrafast tryptic digestion. mAbs 2016, 8 (8), 1477–1486. [PubMed: 27598507]
49. Jakes C; Martin S; Kristensen D; Cook K; Bones J; Carillo S, Enhancing Peptide Mapping Sequence Coverage Through an Automated Dual Protease Digest. LCGC Europe 2023, 36 (07), 246– 254, DOI: 10.56530/lcgc.eu.zq5389j9
50. Ren D; Pipes GD; Liu D; Shih L-Y; Nichols AC; Treuheit MJ; Brems DN; Bondarenko PV, An improved trypsin digestion method minimizes digestion-induced modifications on proteins. Analytical Biochemistry 2009, 392 (1), 12–21. [PubMed: 19457431]
51. Pot S; Gstittner C; Heinrich K; Hoelterhoff S; Grunert I; Leiss M; Bathke A; Domínguez-Vega E, Fast analysis of antibody-derived therapeutics by automated multidimensional liquid chromatography-Mass spectrometry. Anal. Chim. Acta 2021, 1184, 339015 DOI: 10.1016/j.aca.2021.339015 [PubMed: 34625261]
52. Mao Y; Valeja SG; Rouse JC; Hendrickson CL; Marshall AG, Top-Down Structural Analysis of an Intact Monoclonal Antibody by Electron Capture Dissociation-Fourier Transform Ion Cyclotron Resonance-Mass Spectrometry. Analytical Chemistry 2013, 85 (9), 4239–4246. [PubMed: 23551206]
53. Fornelli L; Ayoub D; Aizikov K; Liu X; Damoc E; Pevzner PA; Makarov A; Beck A; Tsybin YO, Top-down analysis of immunoglobulin G isotypes 1 and 2 with electron transfer dissociation on a high-field Orbitrap mass spectrometer. Journal of Proteomics 2017, 159, 67–76. [PubMed: 28242452]
54. Lodge JM; Schauer KL; Brademan DR; Riley NM; Shishkova E; Westphall MS; Coon JJ, Top-Down Characterization of an Intact Monoclonal Antibody Using Activated Ion Electron Transfer Dissociation. Analytical Chemistry 2020, 92 (15), 10246–10251. [PubMed: 32608969]
55. Fornelli L; Srzentić K; Huguet R; Mullen C; Sharma S; Zabrouskov V; Fellers RT; Durbin KR; Compton PD; Kelleher NL, Accurate Sequence Analysis of a Monoclonal Antibody by Top-Down and Middle-Down Orbitrap Mass Spectrometry Applying Multiple Ion Activation Techniques. Analytical Chemistry 2018, 90 (14), 8421–8429. [PubMed: 29894161]
56. Jin Y; Lin Z; Xu Q; Fu C; Zhang Z; Zhang Q; Pritts WA; Ge Y, Comprehensive characterization of monoclonal antibody by Fourier transform ion cyclotron resonance mass spectrometry. mAbs 2019, 11 (1), 106–115. [PubMed: 30230956]
57. Shaw JB; Liu W; Vasil Ev YV; Bracken CC; Malhan N; Guthals A; Beckman JS; Voinov VG, Direct Determination of Antibody Chain Pairing by Top-down and Middle-down Mass Spectrometry Using Electron Capture Dissociation and Ultraviolet Photodissociation. Anal. Chem 2020, 92 (1), 766–773. [PubMed: 31769659]
58. Fornelli L; Ayoub D; Aizikov K; Beck A; Tsybin YO, Middle-Down Analysis of Monoclonal Antibodies with Electron Transfer Dissociation Orbitrap Fourier Transform Mass Spectrometry. Analytical Chemistry 2014, 86 (6), 3005–3012. [PubMed: 24588056]
59. Srzentić K; Nagornov KO; Fornelli L; Lobas AA; Ayoub D; Kozhinov AN; Gasilova N; Menin L; Beck A; Gorshkov MV; Aizikov K; Tsybin YO, Multiplexed Middle-Down Mass Spectrometry as a Method for Revealing Light and Heavy Chain Connectivity in a Monoclonal Antibody. Analytical Chemistry 2018, 90 (21), 12527–12535. [PubMed: 30252447]
60. Srzentić K; Fornelli L; Tsybin YO; Loo JA; Seckler H; Agar JN; Anderson LC; Bai DL; Beck A; Brodbelt JS; Van Der Burgt YEM; Chamot-Rooke J; Chatterjee S; Chen Y; Clarke DJ; Danis PO; Diedrich JK; D'Ippolito RA; Dupré M; Gasilova N; Ge Y; Goo YA; Goodlett DR; Greer S; Haselmann KF; He L; Hendrickson CL; Hinkle JD; Holt MV; Hughes S; Hunt DF; Kelleher NL; Kozhinov AN; Lin Z; Malosse C; Marshall AG; Menin L; Millikin RJ; Nagornov KO; Nicolardi S; Paša-Tolić L; Pengelley S; Quebbemann NR; Resemann A; Sandoval W; Sarin R; Schmitt ND; Shabanowitz J; Shaw JB; Shortreed MR; Smith LM; Sobott F; Suckau D; Toby T;

Weisbrod CR; Wildburger NC; Yates JR; Yoon SH; Young NL; Zhou M, Interlaboratory Study for Characterizing Monoclonal Antibodies by Top-Down and Middle-Down Mass Spectrometry. Journal of the American Society for Mass Spectrometry 2020, 31 (9), 1783–1802. [PubMed: 32812765]

61. Chen B; Lin Z; Zhu Y; Jin Y; Larson E; Xu Q; Fu C; Zhang Z; Zhang Q; Pritts WA; Ge Y, Middle-Down Multi-Attribute Analysis of Antibody-Drug Conjugates with Electron Transfer Dissociation. Analytical Chemistry 2019, 91 (18), 11661–11669. [PubMed: 31442030]
62. Hernandez-Alba O; Houel S; Hessmann S; Erb S; Rabuka D; Huguet R; Josephs J; Beck A; Drake PM; Cianférani S, A Case Study to Identify the Drug Conjugation Site of a Site-Specific Antibody-Drug-Conjugate Using Middle-Down Mass Spectrometry. Journal of the American Society for Mass Spectrometry 2019, 30 (11), 2419–2429. [PubMed: 31429052]
63. Larson EJ; Zhu Y; Wu Z; Chen B; Zhang Z; Zhou S; Han L; Zhang Q; Ge Y, Rapid Analysis of Reduced Antibody Drug Conjugate by Online LC-MS/MS with Fourier Transform Ion Cyclotron Resonance Mass Spectrometry. Analytical Chemistry 2020, 92 (22), 15096–15103. [PubMed: 33108180]
64. Watts E; Williams JD; Miesbauer LJ; Bruncko M; Brodbelt JS, Comprehensive Middle-Down Mass Spectrometry Characterization of an Antibody–Drug Conjugate by Combined Ion Activation Methods. Analytical Chemistry 2020, 92 (14), 9790–9798. [PubMed: 32567851]
65. Wei B; Zenaidee MA; Lantz C; Ogorzalek Loo RR; Loo JA, Towards understanding the formation of internal fragments generated by collisionally activated dissociation for top-down mass spectrometry. Anal. Chim. Acta 2022, 1194, 339400. [PubMed: 35063165]
66. Durbin KR; Skinner OS; Fellers RT; Kelleher NL, Analyzing internal fragmentation of electrosprayed ubiquitin ions during beam-type collisional dissociation. J. Am. Soc. Mass Spectrom 2015, 26 (5), 782–787. [PubMed: 25716753]
67. Zenaidee MA; Lantz C; Perkins T; Jung W; Loo RRO; Loo JA, Internal Fragments Generated by Electron Ionization Dissociation Enhance Protein Top-Down Mass Spectrometry. J. Am. Soc. Mass Spectrom 2020, 31 (9), 1896–1902. [PubMed: 32799534]
68. Lantz C; Zenaidee MA; Wei B; Hemminger Z; Ogorzalek Loo RR; Loo JA, ClipsMS: An Algorithm for Analyzing Internal Fragments Resulting from Top-Down Mass Spectrometry. J. Proteome Res 2021, 20 (4), 1928–1935. [PubMed: 33650866]
69. Schmitt ND; Berger JM; Conway JB; Agar JN, Increasing Top-Down Mass Spectrometry Sequence Coverage by an Order of Magnitude through Optimized Internal Fragment Generation and Assignment. Anal. Chem 2021, 93 (16), 6355–6362. [PubMed: 33844516]
70. Zenaidee MA; Wei B; Lantz C; Wu HT; Lambeth TR; Diedrich JK; Ogorzalek Loo RR; Julian RR; Loo JA, Internal Fragments Generated from Different Top-Down Mass Spectrometry Fragmentation Methods Extend Protein Sequence Coverage. J. Am. Soc. Mass Spectrom 2021, 32 (7), 1752–1758. [PubMed: 34101447]
71. Wei B; Zenaidee MA; Lantz C; Williams BJ; Totten S; Ogorzalek Loo RR; Loo JA, Top-down mass spectrometry and assigning internal fragments for determining disulfide bond positions in proteins. The Analyst 2023, 148 (1), 26–37.
72. Dunham SD; Wei B; Lantz C; Loo JA; Brodbelt JS, Impact of Internal Fragments on Top-Down Analysis of Intact Proteins by 193 nm UVPD. Journal of Proteome Research 2023, 22 (1), 170–181. [PubMed: 36503236]
73. Li H; Sheng Y; Mcgee W; Cammarata M; Holden D; Loo JA, Structural Characterization of Native Proteins and Protein Complexes by Electron Ionization Dissociation-Mass Spectrometry. Anal. Chem 2017, 89 (5), 2731–2738. [PubMed: 28192979]
74. Li H; Nguyen HH; Ogorzalek Loo RR; Campuzano IDG; Loo JA, An integrated native mass spectrometry and top-down proteomics method that connects sequence to structure and function of macromolecular complexes. Nat. Chem 2018, 10 (2), 139–148. [PubMed: 29359744]
75. Rolfs Z; Smith LM, Internal Fragment Ions Disambiguate and Increase Identifications in Top-Down Proteomics. J. Proteome Res 2021, 20 (12), 5412–5418. [PubMed: 34738820]
76. Wei B; Lantz C; Ogorzalek Loo RR; Campuzano IDG; Loo JA In Internal Fragments Enhance Middle-Down Mass Spectrometry Structural Characterization Of Monoclonal Antibodies And

Antibody-Drug Conjugates, 71st ASMS Conference on Mass Spectrometry and Allied Topics, Houston, TX, June 4–8, 2023; Houston, TX.

77. Beaumal C; Deslignière E; Diemer H; Carapito C; Cianférani S; Hernandez-Alba O, Improved characterization of trastuzumab deruxtecan with PTCR and internal fragments implemented in middle-down MS workflows. Analytical and Bioanalytical Chemistry 2023.
78. Clauser KR; Baker P; Burlingame AL, Role of Accurate Mass Measurement (±10 ppm) in Protein Identification Strategies Employing MS or MS/MS and Database Searching. Analytical Chemistry 1999, 71 (14), 2871–2882. [PubMed: 10424174]
79. Marty MT; Baldwin AJ; Marklund EG; Hochberg GKA; Benesch JLP; Robinson CV, Bayesian Deconvolution of Mass and Ion Mobility Spectra: From Binary Interactions to Polydisperse Ensembles. Analytical Chemistry 2015, 87 (8), 4370–4376. [PubMed: 25799115]
80. Alt N; Zhang TY; Motchnik P; Taticek R; Quarmby V; Schlothauer T; Beck H; Emrich T; Harris RJ, Determination of critical quality attributes for monoclonal antibodies using quality by design principles. Biologicals 2016, 44 (5), 291–305. [PubMed: 27461239]
81. Lippold S; Cadang L; Schlothauer T; Yang F, Internal Fragment Ions from Higher Energy Collision Dissociation Enable the Glycoform-Resolved Asn325 Deamidation Assessment of Antibodies by Middle-Down Mass Spectrometry. Analytical Chemistry 2023, 95 (45), 16447–16452. [PubMed: 37903404]
82. Campuzano IDG; Netirojjanakul C; Nshanian M; Lippens JL; Kilgour DPA; Van Orden SL; Loo J, Native-MS Analysis of Monoclonal Antibody Conjugates by Fourier Transform Ion Cyclotron Resonance Mass Spectrometry. Analytical Chemistry 2018, 90 (1), 745–751. [PubMed: 29193956]
83. Michalski A; Neuhauser N; Cox J; Mann M, A systematic investigation into the nature of tryptic HCD spectra. J Proteome Res 2012, 11 (11), 5479–91. [PubMed: 22998608]

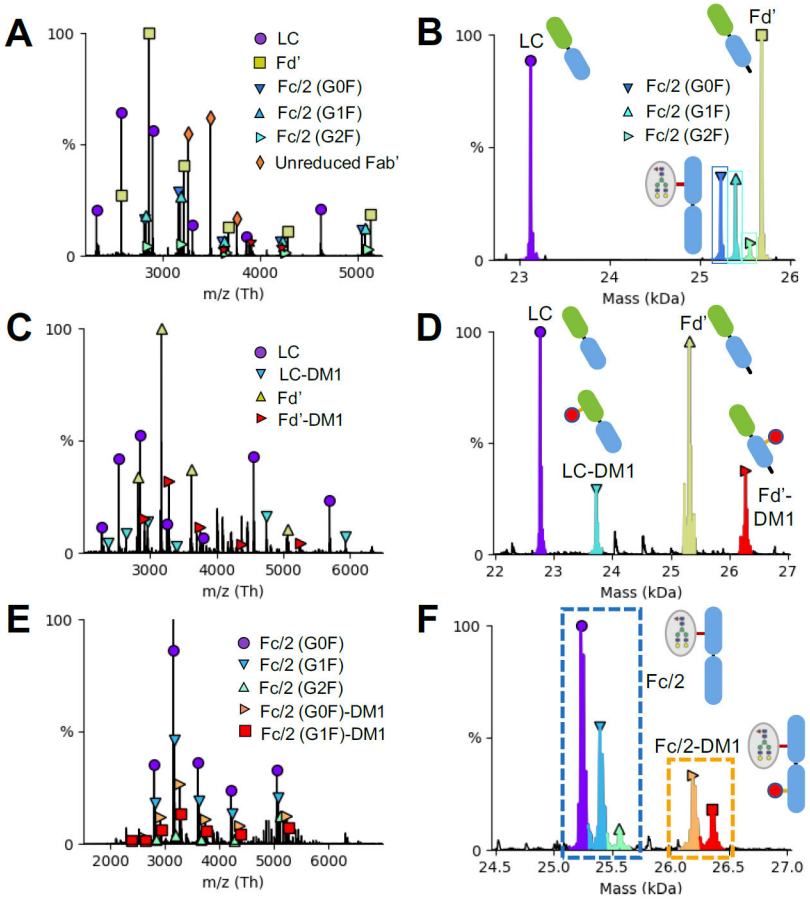

Figure 1.

Native MS spectra of (A) the IdeS/TCEP reduced NIST mAb, (C) the IdeS/TCEP reduced IgG1-DM1 ADC, and (E) the IdeS digested IgG1-DM1 ADC. Deconvolved zero-charged spectra[79] of (B) the IdeS/TCEP reduced NIST mAb, (D) the IdeS/TCEP reduced IgG1-DM1 ADC, and (F) the IdeS digested IgG1-DM1 ADC. All three subunits of the NIST mAb, all three subunits and their DM1-bound forms of the ADC can be separated and observed from our native direct infusion middle-down MS experiments. The heterogeneity of the intact mAb and ADC were well displayed in Figure 1 of our previous report[34], and the need of two individual reduction experiments to separate all subunits and their drug-bound forms of the ADC exemplified its high structural heterogeneity.

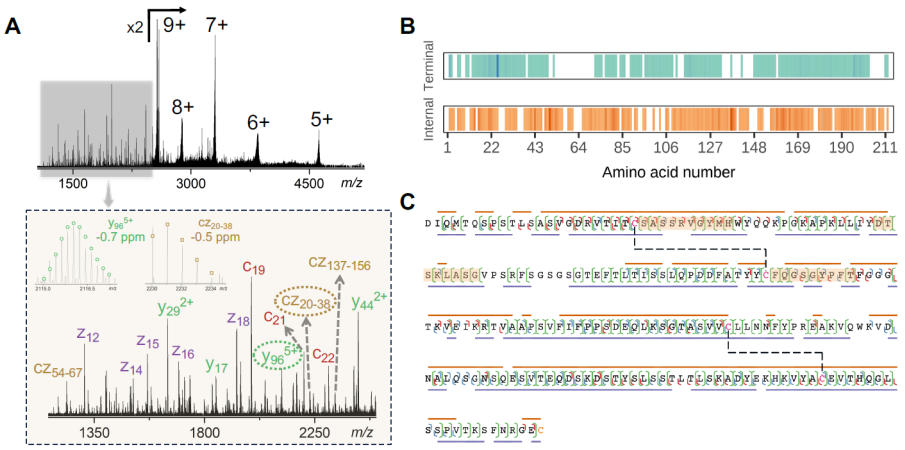

Figure 2.

MD-MS characterization of the NIST mAb LC subunit. (A) A representative ECD MS/MS spectrum of the NIST mAb LC subunit, $[\text{NIST-LC} + 9\text{H}]^{9+}$, with a zoomed-in spectrum in the range from *m/z* 1200 to 2500 showing both terminal and internal fragments are generated. Theoretical isotope distributions are overlaid on representative terminal and internal fragment ions to confirm the assignments. (B) A sequence map showing the sequence coverage achieved by terminal (top panel) and internal (bottom panel) fragments. Deeper color indicates higher fragment intensity on the cleavage site. (C) A fragmentation map showing cleavage sites by terminal and internal fragments. Blue, red, and green cleavages on the protein backbone represent *a* or *b/x* or *y* terminal, c/z· terminal, and cz· internal fragments, respectively. The solid line above the sequence represents terminal fragment sequence coverage, while the solid line beneath the sequence represents internal fragment sequence coverage. The black dashed lines represent intrachain disulfide bonds, with the complementarity-determining regions (CDRs) covered in orange.

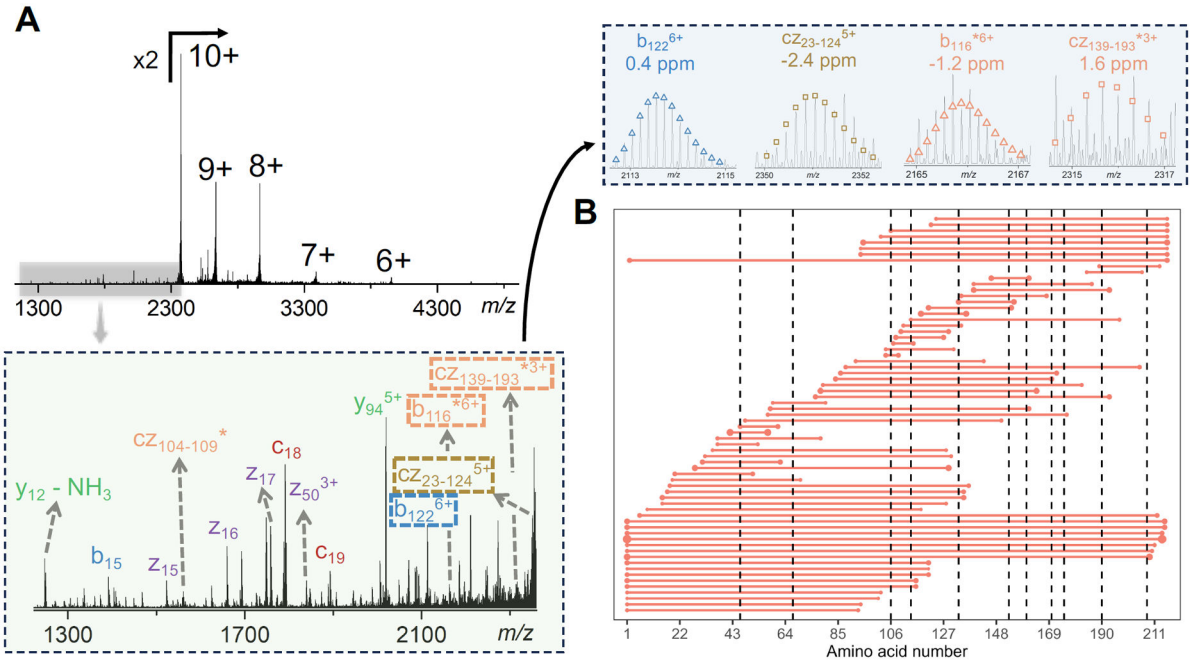

Figure 3.

Middle-down characterization of the IgG1-DM1 ADC LC subunit. (A) A representative ECD MS/MS spectrum of the ADC LC subunit, $[ADC\text{-}LC + 10H]^{10+}$, with a zoomed-in spectrum in the range from 1100 to 2400 *m/z* showing both terminal and internal fragments, and their DM1-bound forms are generated. A superscripted asterisk (*) indicates fragments that contain a DM1 payload. Theoretical isotope distributions are overlaid on representative terminal and internal fragments to confirm the assignments. (B) A fragment location map of the ADC LC subunit showing all DM1-bound fragments after combining ECD data from all isolated charge states. Black vertical dashed lines represent lysine positions.

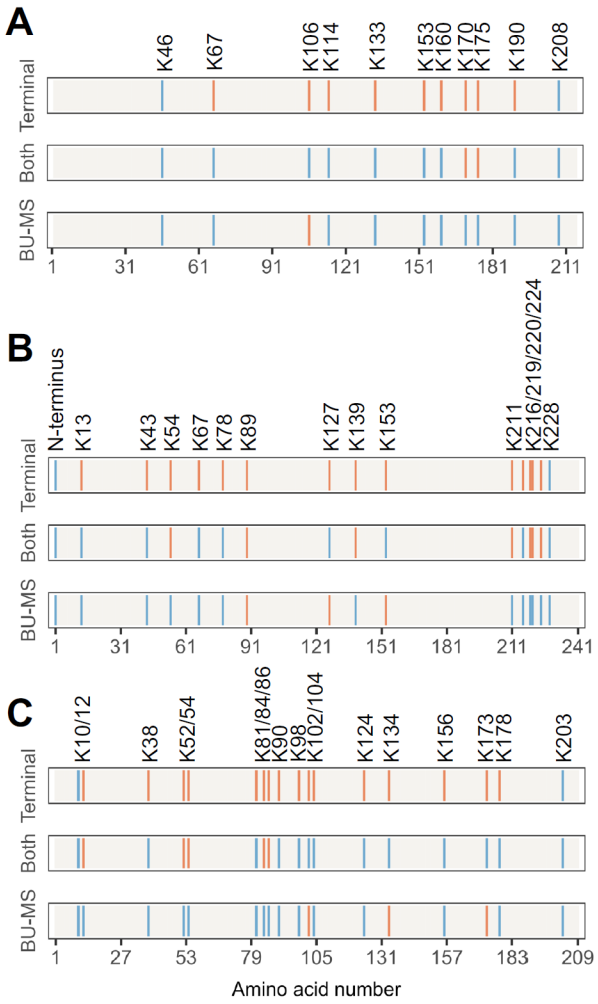

Figure 4.

A sequence map that shows the conjugation determination status of each putative conjugation site for the (A) LC, (B) Fd', and (C) Fc/2 subunit of the IgG1-DM1 ADC with only terminal fragments considered (top row), both terminal and internal fragments considered (middle row), and using bottom-up peptide mapping method (BU-MS, bottom row, data from a previous report[1]). All potential conjugation sites (all K residues and the N-terminus of the Fd' subunit) are highlighted. Orange-colored residues represent *undetermined* conjugation sites and blue-colored residues represent *determined* conjugation sites. A comparison between the middle and bottom rows of each subunit reveals that the determined conjugation sites from MD-MS (this study) and peptide mapping[1] are largely complementary to each other.